Materials Advances

ROYAL SOCIETY OF CHEMISTRY

PAPER

View Article Online
View Journal | View Issue



Cite this: *Mater. Adv.*, 2022, 3, 682

# Competitive induction of circularly polarized luminescence of CdSe/ZnS quantum dots in a nucleotide–amino acid hydrogel†

Xin Wen,[ab] Huahua Fan,[a] Lihong Jing,[a] Ming Deng,[a] Xiaodan Huang,[a] Tifeng Jiao,[b] Li Zhang *[a] and Minghua Liu *[a]

The design and fabrication of chiral inorganic materials with circularly polarized luminescence (CPL) have attracted great interest. Herein, achiral fluorescent quantum dots (QDs) were found to show CPL activity upon doping into the two-component hydrogels composed of *N*-[(9*H*-fluoren-9-ylmethoxy) carbonyl]-glutamic acid (Fmoc-Glu) and deoxyguanosine (dG). It was found that the helical structures could be formed in the two-component hydrogels, and the helicity was dependent on the absolute configuration of Fmoc-Glu. Upon introduction of water-soluble achiral CdSe/ZnS QDs into the hydrogel, the hydrogel could transmit chirality to QDs and make achiral QDs show obvious CPL signals. The mirrored CPL spectra of QDs were obtained when the enantiomeric Fmoc-Glu was used, *i.e.*, negative and positive CPL signals appeared in the L-Fmoc-Glu/dG and D-Fmoc-Glu/dG hydrogels, respectively, which indicated that the CPL signal followed the molecular chirality of Fmoc-Glu. However, when $K^+$ ions were added into the co-assembly of Fmoc-Glu/dG/QDs, only negative CPL signals of QDs could be obtained regardless of whether the L-Fmoc-Glu or D-Fmoc-Glu was used. It was suggested that the G-quadruplex ($G_4$) was formed when $K^+$ ions were introduced into the gel, which is more competitive in inducing the supramolecular chirality of achiral QDs than Fmoc-Glu. This study provides not only a convenient way to fabricate CPL-active QDs *via* gelation, but also a deep understanding on the competitive chirality transfer in the multi-component supramolecular hybrid system.

Received 13th September 2021,
Accepted 13th November 2021

DOI: 10.1039/d1ma00843a

rsc.li/materials-advances



## Introduction

Semiconductor quantum dots (QDs) have attracted considerable attention, mainly due to their excellent properties of narrow and size-tunable emission, high photoluminescence (PL) quantum yields and chemical stability.[1–4] These properties have rendered QDs potential applications on light-emitting devices, solar energy harvesting, photocatalysis, sensing, and imaging.[5–8] In biological applications, water soluble QDs are considered to be biocompatible, opening up great opportunities for their bio-medical applications.[2,9] On the other hand, chirality is a basic property in biological systems. Thus, the development of chiral inorganic materials, such as quantum dots, Au nanoparticles and clusters is a pressing issue in research into the biological system.[10–14] Many works have been reported so far for the fabrication of chiral QDs, which generally showed circular dichroism (CD).[15–19] However, QDs with circularly polarized luminescence (CPL) emission are rarely explored. In these examples, the chiral QDs with CPL emission were achieved mainly in two ways, covalent capping and non-covalent assembly. For the organic capping, chiral ligands such as enantiomeric cysteine, penicillamine and protein were usually used to bind on the surface of QDs and induce the CPL emission.[20–24] The co-assembling achiral quantum dots with chiral matrixes can be developed for the fabrication of CPL-active QDs.[25–30] In the case of chiral molecules capped QDs, the dissymmetry factor or $g_{lum}$, which is an important parameter to measure the performance of CPL activity, is relatively small. Although the co-assembly way increased the $g_{lum}$, CPL-active QDs hybrids were only realized in the organic phases. Here, we reported the hydrogel endowed generation of the CPL activity from the co-assembly of achiral QDs with the chiral hydrogels.

Derivatives of amino acids and nucleotides are the basic building-block components of the organisms. Meanwhile, they are also the important building blocks for the formation of diverse chiral assemblies, as they have multiple hydrogen-bond

[a] *Beijing National Laboratory for Molecular Science (BNLMS), CAS Key Laboratory of Colloid, Interface and Chemical Thermodynamics, Institute of Chemistry, Chinese Academy of Sciences, Beijing 100190, P. R. China. E-mail: zhangli@iccas.ac.cn, liumh@iccas.ac.cn*
[b] *Hebei Key Laboratory of Applied Chemistry, School of Environmental and Chemical Engineering, Yanshan University, Qinhuangdao 066004, P. R. China*

† Electronic supplementary information (ESI) available: SEM images, AFM images and UV-Vis spectra. See DOI: 10.1039/d1ma00843a

donor/acceptor sites and chiral centres within their molecular structures.[31–39] Thus, the co-assemblies from amino acid and nucleotides derivatives with QDs are expected to be a good approach for inducing CPL signals of water soluble quantum dots.[26] Previously, we achieved the hydrogelation of Fmoc-Glu and purine nucleobases and obtained helical nanostructures.[31] Herein, we desired to develop an approach for rendering QDs with CPL emission using these chiral supramolecular structures in aqueous system. It was found that the enantiomers of Fmoc-Glu could form two-component hydrogels with D-deoxynucleotides, respectively. The chirality transfer coming from co-assemblies with QDs to generate the CPL was explored. Since the co-assembly contained two kinds of chiral components, we intended to further understand which one would determine the induced CPL signals of QDs. In addition, upon addition of $K^+$ ions, it has been known that dG could form a G-quadruplex stabilized by $K^+$ ions.[40,41] In this case, what would happen to the CPL signals of QDs in the complex assemblies composed of multi-components? To understand the chirality transfer in the complicated assemblies, we chose CdSe/ZnS QDs with green emission as a model material to study the CPL emission. The CPL induction of the QDs by the hydrogels composed of Fmoc-Glu and D-deoxynucleotides was investigated in the absence and presence of $K^+$ ions, respectively. Scheme 1 shows the induced CPL of QDs in the co-assemblies of Fmoc-Glu and dG. The co-gels with obvious CPL emission could be obtained in the co-assemblies containing Fmoc-Glu, dG and QDs, and the CPL signals followed the configuration of Fmoc-Glu in the absence of $K^+$ ions. Upon addition of $K^+$ ions, however, the negative CPL signal was always presented regardless of the absolute configuration of Fmoc-Glu changed. This means that in the absence of $K^+$ ions, the Fmoc-Glu assemblies determined the CPL generation of the QDs. In the presence of $K^+$ ions, where the G-quadruplex was formed, $G_4$ determined the CPL activity. So far, although the induction of CPL of achiral QDs was reported in the organic media, here, we showed the example that CPL active QDs formed in the hydrogel. Remarkably, a competitive chiral induction by the amino acids and nucleotides was reported for the first time.

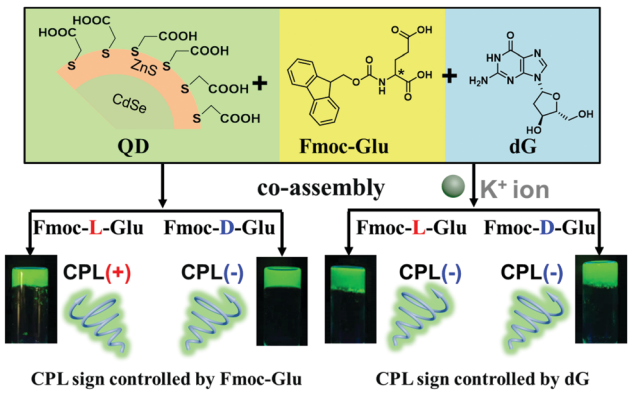


Scheme 1 Illustration on the induced CPL signals of CdSe/ZnS QDs obtained in the hydrogels of Fmoc-Glu and dG. In the Fmoc-Glu/dG hydrogels, the CPL signal of QDs followed the absolute configuration of Fmoc-Glu; in the presence of $K^+$ ions, the CPL signals were determined by dG.

# Results and discussion

## Hydrogels of Fmoc-Glu and deoxynucleotides

The assembling behaviours of Fmoc-Glu (L- or D-enantiomers) and D-deoxynucleotides were investigated by mixing them in water and cooling to room temperature after heating. Although Fmoc-Glu itself could not form hydrogels,[34] translucent hydrogels were formed by co-assembling with the deoxyguanosine (dG) and deoxyadenosine (dA), respectively. For pyrimidine nucleosides, deoxythymidine (dT) and deoxycytidine (dC) could not afford a stable hydrogel with Fmoc-Glu (Fig. S1, ESI†).

Morphology and spectral information were characterized by scanning electron microscopy (SEM), atomic force microscopic (AFM), UV-Vis and circular dichroism (CD) spectroscopy. As shown in Fig. 1a, b and Fig. S2a (ESI†), left-handed helical structures were observed in the L-Fmoc-Glu/dG co-gel, while the right-handed helices were obtained in the D-Fmoc-Glu/dG co-gel. These helices had a pitch around 110 nm and width around 50 nm. Furthermore, the L-Fmoc-Glu/dG co-assembly showed a positive Cotton effect in the region of 255–330 nm (Fig. 1e, black line), in accordance with the absorption spectrum (Fig. S3, ESI,† green line), which was assigned to the π–π* transition of the Fmoc chromophore,[42,43] and then the CD spectrum of D-Fmoc-Glu/dG showed a mirror image (negative signal) compared to that of L-Fmoc-Glu/dG (Fig. 1e, red line). The results of CD spectra were consistent with those observed by SEM images, indicating that the helicity of nanostructures was dependent on the molecular chirality of Fmoc-Glu. In addition, L-Fmoc-Glu/dA exhibited left-handed nanostructures

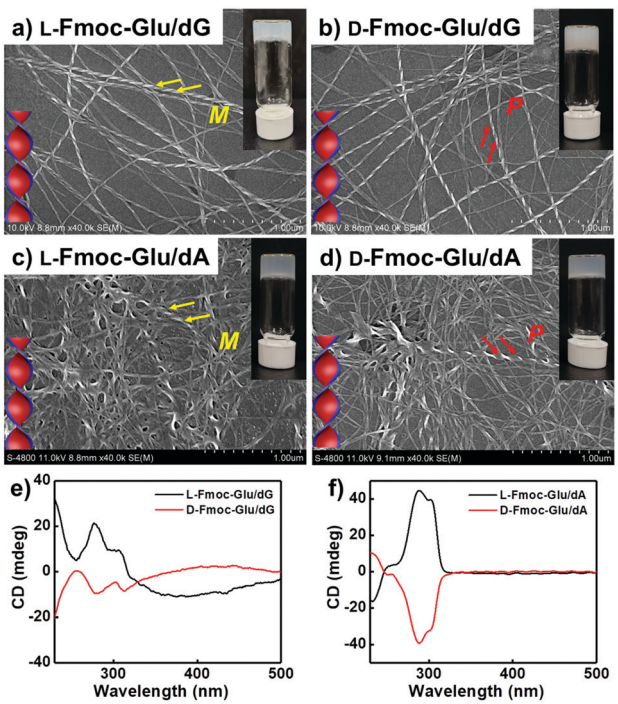


Fig. 1 (a and b) SEM images and (e) CD spectra of the hydrogels of L(D)-Fmoc-Glu/dG. (c and d) SEM images and (f) CD spectra of the hydrogels of L(D)-Fmoc-Glu/dA.

and a positive CD signal, which were both opposite to the D-Fmoc-Glu/dA co-assembly, showing similar structures and spectral characteristics compared to the L- or D-Fmoc-Glu/dG co-assemblies (Fig. 1c, d, f and Fig. S2b, ESI†). There were no regular and obvious helical nanostructures in the co-assemblies of Fmoc-Glu/dT (or dC) (Fig. S1, ESI†), indicating the interaction between Fmoc-Glu and dT (or dC) too weak to form stable hydrogels and the corresponding chiral structures. These results indicated that dG (or dA), which had the stronger intermolecular interaction with Fmoc-Glu, could induce the more effective stacking of Fmoc-Glu, thus producing chiral nanostructures and chiral spectral signals compared with dT (or dC). Moreover, these stable hydrogels composed of Fmoc-Glu/dG (or dA) could be applied to transfer its chirality to luminescent quantum dots.

### Hydrogels of Fmoc-Glu and dG/dA upon addition of $K^+$ ions

It was known that guanosine-based derivatives self-associated into G-quadruplexes, which were composed with an arrangement of four guanine moieties connected together by eight hydrogen-bonding interactions and stabilized by $K^+$ ions, and then the G-quartets stacked to form stable G-quadruplexes ($G_4$).[34,44–50] However, it has been demonstrated that high-order aggregates for adenosine or deoxyadenosine upon addition of any alkali metal were unable to form.[51] Thus, the $K^+$ ions were introduced into the system of Fmoc-Glu/dG and Fmoc-Glu/dA co-gels. Steady hydrogels were still formed in the mixture of Fmoc-Glu and dG/dA involving $K^+$ ions. The morphology and chiroptical properties of these systems were further investigated using SEM images and CD spectra (Fig. 2). It was interesting to find that the helical nanostructures in the hydrogels of Fmoc-Glu/dG/$K^+$ (both L and D enantiomer) nearly disappeared (Fig. 2a and b), while the helices in the hydrogel of Fmoc-Glu/dA/$K^+$ were retained in accordance with the situation without $K^+$ ions (Fig. 2c and d). Thus, we speculated that the formation of the G-quadruplex might lead to the formation of nanoribbons. Meanwhile, the CD spectra of L- and D-Fmoc-Glu/dG/$K^+$ were no longer mirrored images, as shown in Fig. 2e, while that of L- and D-Fmoc-Glu/dA/$K^+$ still exhibited mirror-imaged CD spectra (Fig. 2f). The CD spectrum of L-Fmoc-Glu/dG/$K^+$ showed positive Cotton effect in the region of 260–360 nm, and D-Fmoc-Glu/dG/$K^+$ also exhibited positive Cotton effect around this range, indicating that the chirality of Fmoc-Glu was not the only factor that determined the CD signals. As shown in Fig. S4 (ESI†), the CD spectrum of dG/$K^+$ (4 mM/1 mM) showed a positive peak at around 300 nm, which was similar to the CD spectrum of the quadruplex.[52,53] Then, the positive Cotton effect of L- and D-Fmoc-Glu/dG/$K^+$ in the region of 300–320 nm might be ascribed to the formation of the G-quadruplex in the multi-component hydrogels in the presence of $K^+$ ions. It should be noted that, compared with Fig. 1f and 2f, the CD spectra of Fmoc-Glu/dA/$K^+$ barely changed upon adding $K^+$ ions since dA was unable to form high-order aggergates.[48] This implied that in the presence of $K^+$ ions, the G-quadruplex was possibly formed, which would contribute predominantly to the CD spectra.

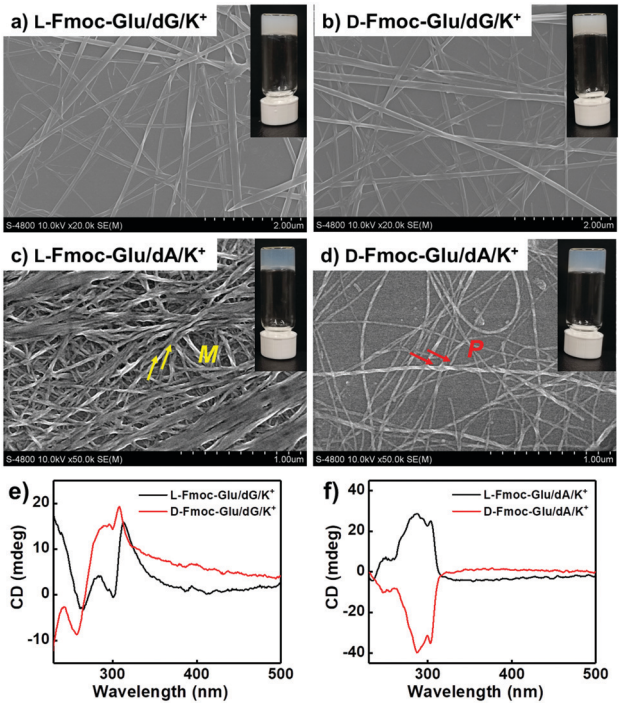


Fig. 2 (a and b) SEM images and (e) CD spectra of the hydrogels of L(D)-Fmoc-Glu/dG/$K^+$. (c and d) SEM images and (f) CD spectra of the hydrogels of L(D)-Fmoc-Glu/dA/$K^+$.

### Chirality transfer to QDs and CPL signal control

The above-mentioned hydrogels were further used as a matrix to transfer their chirality to achiral CdSe/ZnS QDs. All QDs-doped hydrogels appeared to be stable without precipitation. The QDs in the hydrogels and in the aqueous solution exhibited the similar photoluminescence quantum yield (PLQY) (Table S1, ESI†), indicating the gels could serve as templates to transfer the chirality to QDs without sacrificing PLQY. Compared with the QDs solution, the luminescence lifetime of QDs decreased after doped into hydrogels (Table S2, ESI†), which was probably due to the interaction of the QDs with the gelators. As shown in Fig. 3a, in which COOH-modified achiral QDs co-assembled with Fmoc-Glu and dG, the positive and the negative CPL signals were detected from the gel containing L-Fmoc-Glu/dG and D-Fmoc-Glu/dG, respectively. The result implied that when the helices of Fmoc-Glu/dG (L and D, respectively) were used as templates, the chirality of the assemblies was successfully transferred to achiral QDs, which emitted mirrored CPL at 533 nm. In this co-assembling state, the QDs showed a slight redshift from 529 nm to 533 nm, in comparison with the fluorescence spectrum of the QDs solution (Fig. S5, ESI†), and we attributed it to the slight aggregation of QDs.[54] When we measured the chiroptical properties of the dispersion of the Fmoc-Glu/QDs mixtures without the addition of dG (note that Fmoc-Glu itself could not form a hydrogel). As shown in Fig. S6 (ESI†), no CPL signal was observed in the mixed dispersion of Fmoc-Glu/QDs. This result indicated that the signal Fmoc-Glu component could not induce the CPL signals of QDs. Furthermore, we investigated the CPL signals of QDs in Fmoc-Glu/dG when the concentration of Fmoc-Glu/dG was too low

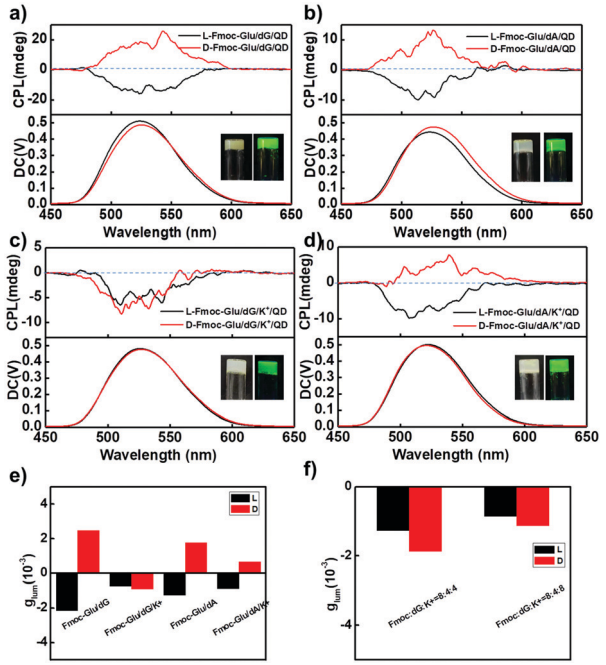


Fig. 3 CPL spectra of QDs-doped hydrogels for (a) Fmoc-Glu/dG/QD; (b) Fmoc-Glu/dA/QD; (c) Fmoc-Glu/dG/$K^+$/QD; (d) Fmoc-Glu/dA/$K^+$/QD. (e) Summary $g_{lum}$ values of QD-doped hydrogels according to a–d. (f) Summary $g_{lum}$ values of QD-doped hydrogels of Fmoc-Glu/dG/$K^+$/QD with different $K^+$ ion ratios.

to form a hydrogel. No CPL signal was detected when the concentration of Fmoc-Glu was 2 mM and 1 mM, in which the hydrogels were not formed (Fig. S7, ESI†). These results further indicated that the hydrogelation or the forming of the formed chiral nanostructures was necessary to serve effective matrices to transfer chirality to QDs.

Furthermore, as the concentration of QDs doped into hydrogel increased, the intensity of CPL signals gradually increased and finally achieved saturation. As shown in Fig. S8 (ESI†), there was almost no CPL signal when only 1 nM QDs were added into the hydrogels. As the concentration of QDs increased, the $g_{lum}$ values gradually increased and reached a plateau. Here, we selected 20 nM as a suitable concentration to carry out the following experiment. After addition of QDs into the Fmoc-Glu/dG co-gels, similar helical nanostructures were well retained as shown in Fig. S9 (ESI†), and the handedness of the helical nanostructures was maintained. The TEM image indicated that QDs gathered on the surface of the helices (insert in Fig. S9a, ESI†). It has been suggested that the chirality of the QDs could originate from the chiral molecules inducing induction on the surface, electronic interactions induced by large dipole moments between the chiral molecules and achiral structure, and the achiral QDs-based chiral self-assembly.[20–30] Here, we speculated that the interaction between the QDs and gelator molecules, as well as the arrangement of QDs, could be the main origin of the induced chirality of the QDs.[25]

It was found that mirrored CPL spectra were generated in the hydrogels of Fmoc-Glu/dA (L and D), and positive and negative CPL signals were obtained at 533 nm when L- and D-enantiomers of Fmoc-Glu were used, respectively (Fig. 3b). These results indicated that the CPL signals of QDs followed the chirality of Fmoc-Glu, *i.e.*, the L-enantiomer of Fmoc-Glu gave negative CPL signals and the D-enantiomer gave positive CPL signals.

To exploit the hydrogels upon addition of $K^+$ ions as templates to transfer chirality, we measured CPL of QDs-doped hydrogels of Fmoc-Glu/dG/$K^+$ and Fmoc-Glu/dA/$K^+$. The preparation of the hydrogel containing $K^+$ ions was as follows: $K^+$ ions were mixed with Fmoc-Glu, dG and QDs in the aqueous solution, which was heated and cooled until a stable hydrogel was formed. It was found that negative CPL signals were observed in either L- or D-Fmoc-Glu/dG/$K^+$ systems, which were no longer mirrored CPL signals (Fig. 3c). In contrast, obvious mirrored CPL signals were obtained for QDs in the hydrogels of Fmoc-Glu/dA/$K^+$ (L and D), as shown in Fig. 3d. Furthermore, Fig. 3e summarizes the $g_{lum}$ in various hydrogels, and both negative signals were observed in the QDs-doped L- and D-Fmoc-Glu/dG/$K^+$, suggesting that the CPL signals in that case were determined by the formation of the G-quadruplex even if a pair of Fmoc-Glu enantiomers participated in the assembling process. The CD spectrum of D-Fmoc-Glu/dG/QD showed a mirror image compared to that of L-Fmoc-Glu/dG/QD, while the CD spectra of L- and D-Fmoc-Glu/dG/$K^+$/QD were no longer a mirrored image, and these results were consistent with the spectra without QDs (Fig. S10, ESI†). To further illustrate the effect of $K^+$ ions in stabilizing the formation of G-quadruplex and then to control the CPL signals of QDs, different molar ratios of $K^+$ ions were used to investigate the chirality transfer, as shown in Fig. 3f. We have found that only negative CPL signals were obtained at all molar ratios of $K^+$ ions, further supporting that the generation of the G-quadruplex upon addition of $K^+$ ions was an essential factor to control the CPL signals.

In order to confirm the effectiveness of the chirality transfer and CPL signal control in the multi-component hydrogels, we also tested the CPL spectra of the $NH_2$-protected QDs in the Fmoc-Glu/dG and Fmoc-Glu/dG/$K^+$ co-gels, as shown in Fig. 4, which showed negative CPL signals of $NH_2$-modified QDs in the L-Fmoc-Glu/dG gels, and a positive signal was obtained in the case of the D-Fmoc-Glu/dG gels. The mirrored images of the CPL spectra suggested that the CPL signal of $NH_2$-protected QDs also followed the chirality of Fmoc-Glu. Upon addition of $K^+$ ions, only negative CPL signals could be detected regardless

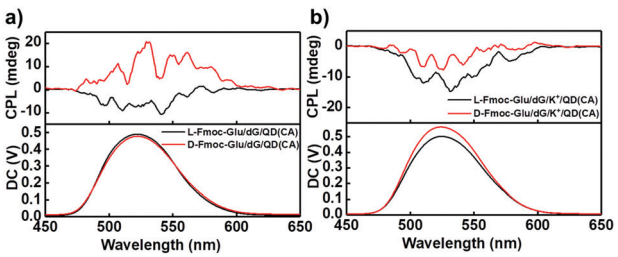


Fig. 4 (a and b) CPL spectra of hydrogels-doped $NH_2$-protected CdSe/ZnS QDs (cysteamine, CA, as ligand). (a) L(D)-Fmoc-Glu/dG/QD(CA). (b) L(D)-Fmoc-Glu/dG/$K^+$/QD(CA).

of whether L-Fmoc-Glu or D-Fmoc-Glu was used to form a hydrogel with dG, presenting the similar result with that of the COOH-protected QDs, also confirming that the G-quadruplex determined the final CPL signal of QDs in the multi-component hydrogels (Fig. 4b).

To further confirm the formation of the G-quadruplex in the multi-component hydrogels, the X-ray diffraction (XRD) patterns were measured for various hydrogels and are illustrated in Fig. 5 and Fig. S11 (ESI†). According to XRD analysis, the samples of the Fmoc-Glu/dG assemblies displayed *d*-spacing of 2.40, 1.20, 0.80, 0.60, 0.48 and 0.40 nm, calculated from Bragg's equation, which corresponded to ratios of 1, 1 : 2, 1 : 3, 1 : 4, 1 : 5 and 1 : 6, respectively, indicating an obvious lamellar structure with a *d*-spacing of 2.40 nm (Fig. 5a).[55] A previous publication has reported that Fmoc-Glu itself displayed a lamellar structure with a *d*-spacing of 2.36 nm and formed a bilayer structure of Fmoc-Glu with the Fmoc moieties stacked.[33] In the two-component hydrogel of Fmoc-Glu/dG, the *d*-spacing value was slightly larger than that of Fmoc-Glu itself, which was the same case as that of Fmoc-Glu/dA. We deemed that the deoxynucleotides were inserted into the bilayer structure and served as a basic repeat unit, which formed multiple bilayers and further hierarchically self-assembled into higher level nanohelices. dG and dA triggered Fmoc-Glu into chiral structures and the supramolecular chirality depended on the molecular chirality of Fmoc-Glu. After blending QDs, the CPL-active hydrogels were obtained by chiral arrangement of QDs and the handedness of CPL was controlled by the molecular chirality of Fmoc-Glu.

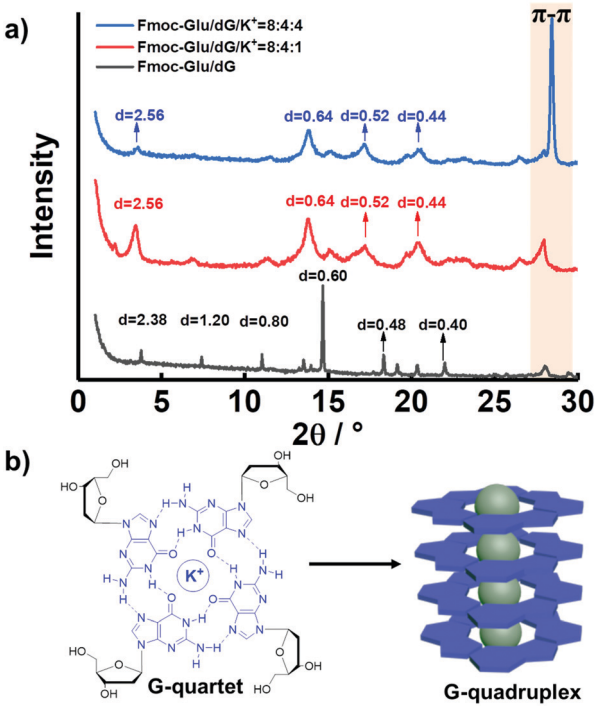


Fig. 5 (a) XRD patterns of hydrogels of Fmoc-Glu/dG, Fmoc-Glu/dG/$K^+$ (8 : 4 : 1, molar ratio) and Fmoc-Glu/dG/$K^+$ (8 : 4 : 4, molar ratio). (b) Formation and stacking of G-quartets.

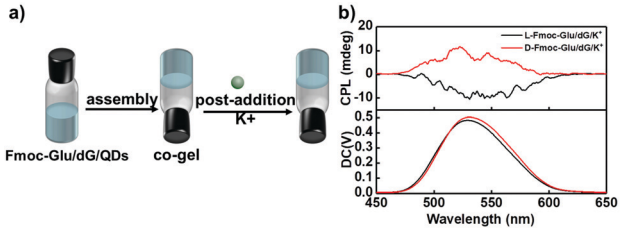


Fig. 6 (a) Schematic representation presenting the procedure with blending $K^+$ ions into gelation. The initial solution contained three components of Fmoc-Glu, dG and QDs. (b) CPL spectra of QDs-doped hydrogels of Fmoc-Glu/dG/$K^+$ with post-addition.

Upon introduction of $K^+$ ions, the XRD patterns of the hydrogels showed an enhanced peak corresponding to 0.32 nm (Fig. 5a, red line and blue line), a value that was in line with the π–π stacking distance between G-quartets.[56] Thus, we hypothesized that the additional $K^+$ ions was able to promote the formation of the G-quartets (Fig. 5b). The enhanced peak corresponding to 0.32 nm (blue line), upon addition of further $K^+$ ions molar ratio, was presumably the result of the increased stabilization of the G-quartets and enhancement of π–π stacking. It was worthy to note that the XRD data of the Fmoc-Glu/dA/$K^+$ hydrogels no longer showed a clear peak at around 0.32 nm, which further confirmed the absence of π–π stacking interactions and the formation of high-order aggregates (Fig. S11, ESI†). On account of the only negative CPL signals presented, we speculated that the formation of the G-quadruplex regulated the CPL signal for QDs. In contrast, dA was unable to form assemblies similar to $G_4$ upon the addition of $K^+$ ions,[45] and thus could not change the CPL signal of QDs. This implied that $G_4$ has stronger ability to transfer the chirality to the QDs.

Such predominant chirality transfer ability of $G_4$ to QDs was further supported by the effect of the formation of the G-quadruplex on the chiral transfer to QDs. We further changed the sequence upon addition of $K^+$ ions into the hydrogels, as shown in Fig. 6a. Fmoc-Glu, dG and QDs first co-assembled to form hydrogels followed by the addition of $K^+$ ions. In this case, the $K^+$ ions were added after the gelation, rather than the addition in the gelation process. Without experiencing of the heating–cooling process, $G_4$ was not formed even in the presence of the $K^+$ ions. In this case, the induced CPL signals of QDs in the hydrogels exhibited mirrored images, *i.e.*, L-Fmoc-Glu/dG/$K^+$ presented a negative signal and D-type Fmoc-Glu gave a positive signal, which follows the Fmoc-Glu assemblies rather than dG (Fig. 6b). This further supported that $G_4$ was responsible for the competitive chirality transfer in the multi-component gel system.

## Experimental

### Materials

*N*-[(9*H*-fluoren-9-ylmethoxy)carbonyl]-L-glutamic acid (L-Fmoc-glutamic acid, >98%), *N*-[(9*H*-fluoren-9-ylmethoxy)carbonyl]-D-glutamic acid (D-Fmoc-glutamic acid, >98%), 2′-deoxyadenosine

(dA, 99%), 2′-deoxycytidine (dC, 99%) and 2′-deoxythymidine (dT, 99%) were purchased from TCI. 2′-Deoxyguanosine (dG, 99%) was purchased from Aladdin. Potassium chloride (KCl, 99.5%) was purchased from Beijing Chemicals. Water soluble CdSe/ZnS quantum dots (CdSe/ZnS QDs) were purchased from Suzhou Xingshuo Nanotech Co., Ltd. All materials were used without further purification. All aqueous solutions were prepared using Milli-Q water (18.2 MΩ·cm) in this investigation.

### Characterization

Circular dichroism (CD) spectra were obtained using a JASCO 1500 spectrophotometer. The UV-Vis spectra were obtained on the SHIMADZU UV-2600 UV-Vis absorption spectrometer. Fluorescence spectra were measured on a F-4500 fluorescence spectrophotometer. Circularly polarized luminescence (CPL) spectra were obtained using a JASCO CPL-200 spectrophotometer. Scanning electron microscopy (SEM) was performed on a Hitachi S-4800 FE-SEM instrument with an accelerating voltage of 10 kV. SEM samples were prepared as follows: a small amount of samples were spread on silicon wafers and dried in a vacuum desiccator. Before SEM measurements, the samples on silicon wafers were coated with a thin layer of Pt to increase the contrast. X-ray diffraction (XRD) analysis was performed on a Rigaku D/Max-2500, Japan X-ray diffractometer (Japan) with Cu Kα radiation ($\lambda$ = 1.54 Å), operated at a voltage of 45 kV and a current of 100 mA. Atomic force microscopic (AFM) images were recorded with a Dimension FastScan (Bruker) instrument in tapping mode, and samples were prepared on mica flakes. For transmission electron microscopy (TEM), a sample was dispersed in water, and several microliters of dispersion solution were spread onto carbon coated Cu grids (unstained), which was vacuum dried for transmission electron microscopy observation on a HT7700 (Hitachi) apparatus with an accelerating voltage of 100 kV. The absolute fluorescence quantum yield was measured by using an absolute PL quantum yield spectrometer FluoroMax+ (HORIBA) with a calibrated integrating sphere. The excitation wavelength was 360 nm and the light path was 2 mm. An Edinburg FLS980 series of fluorescence spectrometers was used to measure the fluorescence decay of the sample by using time-correlated single photon counting (TCSPC) mode.

### Preparation of the hydrogels

All hybrid hydrogels were prepared in a closed glass vial (volume, 4 mL). L(D)-Fmoc-Glu and dG/dA were placed into a glass vial with 1 mL of aqueous solution and the mixture was heated until the solids were completely dissolved, then spontaneous cooled to room temperature (25 °C) and incubated for about 1 hour at least. Finally, we kept the concentration of the L(D)-Fmoc-Glu and the dG/dA at 8 mM and 4 mM, respectively. The formation of the hydrogels was confirmed by vial inversion photos. For the hybrid hydrogels containing $K^+$, different volumes of KCl solution (100 mM) were added to keep the concentration of $K^+$ at 1 mM, 4 mM and 8 mM. To obtain the co-assembled hydrogels containing QDs, we used water soluble CdSe/ZnS QDs to keep its concentration increasing from $1 \times 10^{-9}$ M (1 nM) to $1 \times 10^{-7}$ M (100 nM). The ligand of the QDs is always thioglycollic acid unless otherwise specified.

## Conclusions

In conclusion, chiral QDs materials with CPL emission were successfully prepared, which were fulfilled through encapsulating QDs into the chiral hydrogels in the way of supramolecular co-assembly. We took advantage of Fmoc-Glu co-assembling into hydrogels with dG and dA, and helical architectures were obtained. The chiral assemblies were demonstrated to transfer chirality to achiral QDs to endow QDs with CPL emission. Furthermore, the CPL signal of QDs in the two-component gels followed the molecular chirality of Fmoc-Glu. In addition, when $K^+$ ions were introduced into the Fmoc-Glu/dG systems, the G-quadruplex constituted by dG and $K^+$ ions could act as a bridge to mediate chirality transfer from hydrogels to QDs, which made QDs only possess negative CPL signals. The results demonstrated that the G-quadruplex played an essential role in controlling the CPL signal of QDs. This work not only afforded a method to fabricate chiral inorganic materials in chiral supramolecular hydrogels matrices, but also provided insight on chirality control in the complicated biological systems.

## Conflicts of interest

There are no conflicts to declare.

## Acknowledgements

The authors gratefully acknowledge financial support from the National Natural Science Foundation of China (21890734, 21890730 and 21972150) and the Chinese Academy of Sciences (QYZDJSSW-SLH044).

## References

1 K. E. Knowles, K. H. Hartstein, T. B. Kilburn, A. Marchioro, H. D. Nelson, P. J. Whitham and D. R. Gamelin, *Chem. Rev.*, 2016, **116**, 10820–10851.
2 L. Jing, S. V. Kershaw, Y. Li, X. Huang, Y. Li, A. L. Rogach and M. Gao, *Chem. Rev.*, 2016, **116**, 10623–10730.
3 C. R. Kagan, L. C. Bassett, C. B. Murray and S. M. Thompson, *Chem. Rev.*, 2021, **121**, 3186–3233.
4 X. Gao, B. Han, X. Yang and Z. Tang, *J. Am. Chem. Soc.*, 2019, **141**, 13700–13707.
5 C. Hao, R. Gao, Y. Li, L. Xu, M. Sun, C. Xu and H. Kuang, *Angew. Chem., Int. Ed.*, 2019, **58**, 7371–7374.
6 L. Jing, K. Ding, S. V. Kershaw, I. M. Kempson, A. L. Rogach and M. Gao, *Adv. Mater.*, 2014, **26**, 6367–6386.
7 C. Hao, L. Xu, H. Kuang and C. Xu, *Adv. Mater.*, 2020, **32**, 1802075.

8 J. M. Pietryga, Y.-S. Park, J. Lim, A. F. Fidler, W. K. Bae, S. Brovelli and V. I. Klimov, *Chem. Rev.*, 2016, **116**, 10513–10622.
9 T. He, X. Qiu, J. Li, G. Pang, Z. Wu, J. Cheng, Z. Zhou, J. Hao, H. Liu, Y. Ni, L. Li, X. Lin, W. Hu, K. Wang and R. Chen, *Nanoscale*, 2019, **11**, 15245–15252.
10 Z. Xie, P. Sun, Z. Wang, H. Li, L. Yu, D. Sun, M. Chen, Y. Bi, X. Xin and J. Hao, *Angew. Chem., Int. Ed.*, 2020, **59**, 9922–9927.
11 G. Gonzalez-Rubio, J. Mosquera, V. Kumar, A. Pedrazo-Tardajos, P. Llombart, D. M. Solis, I. Lobato, E. G. Noya, A. Guerrero-Martinez, J. M. Taboada, F. Obelleiro, L. G. MacDowell, S. Bals and L. M. Liz-Marzan, *Science*, 2020, **368**, 1472–1477.
12 L. Xiang, X. Lu, C. Shen, Y. Ke and Q. Wang, *J. Am. Chem. Soc.*, 2014, **137**, 457–462.
13 S. Wang, L. Zheng, W. Chen, L. Ji, L. Zhang, W. Lu, Z. Fang, F. Guo, L. Qi and M. Liu, *CCS Chem.*, 2020, **2**, 2473–2784.
14 W. Ma, L. Xu, A. F. de Moura, X. Wu, H. Kuang, C. Xu and N. A. Kotov, *Chem. Rev.*, 2017, **117**, 8041–8093.
15 X. Gao, X. Zhang, K. Deng, B. Han, L. Zhao, M. Wu, L. Shi, J. Lv and Z. Tang, *J. Am. Chem. Soc.*, 2017, **139**, 8734–8739.
16 M. P. Moloney, J. Govan, A. Loudon, M. Mukhina and Y. K. Gun'ko, *Nat. Protoc.*, 2015, **10**, 558–573.
17 R. Zhou, K. Y. Wei, J. S. Zhao and Y. B. Jiang, *Chem. Commun.*, 2011, **47**, 6362–6364.
18 Z. Zhu, J. Guo, W. Liu, Z. Li, B. Han, W. Zhang and Z. Tang, *Angew. Chem., Int. Ed.*, 2013, **52**, 13571–13575.
19 V. Kuznetsova, Y. Gromova, M. Martinez-Carmona, F. Purcell-Milton, E. Ushakova, S. Cherevkov, V. Maslov and Y. K. Gun'ko, *Nanophotonics*, 2021, **10**, 797–824.
20 M. Naito, K. Iwahori, A. Miura, M. Yamane and I. Yamashita, *Angew. Chem., Int. Ed.*, 2010, **49**, 7006–7009.
21 U. Tohgha, K. K. Deol, A. G. Porter, S. G. Bartko, J. K. Choi, B. M. Leonard, K. Varga, J. Kubelka, G. Muller and M. Balaz, *ACS Nano*, 2013, **7**, 11094–11102.
22 J. Cheng, J. Hao, H. Liu, J. Li, J. Li, X. Zhu, X. Lin, K. Wang and T. He, *ACS Nano*, 2018, **12**, 5341–5350.
23 J. Hao, Y. Li, J. Miao, R. Liu, J. Li, H. Liu, Q. Wang, H. Liu, M. H. Delville, T. He, K. Wang, X. Zhu and J. Cheng, *ACS Nano*, 2020, **14**, 10346–10358.
24 J. Hao, F. Zhao, Q. Wang, J. Lin, P. Chen, J. Li, D. Zhang, M. Chen, P. Liu, M. H. Delville, T. He, J. Cheng and Y. Li, *Adv. Opt. Mater.*, 2021, **9**, 2101142.
25 S. Huo, P. Duan, T. Jiao, Q. Peng and M. Liu, *Angew. Chem., Int. Ed.*, 2017, **56**, 12174–12178.
26 C. Hao, Y. Gao, D. Wu, S. Li, L. Xu, X. Wu, J. Guo, M. Sun, X. Li, C. Xu and H. Kuang, *Adv. Mater.*, 2019, **31**, 1903200.
27 Y. Wang, K. Wan, F. Pan, X. Zhu, Y. Jiang, H. Wang, Y. Chen, X. Shi and M. Liu, *Angew. Chem., Int. Ed.*, 2021, **60**, 16615–16621.
28 Y. Ru, L. Sui, H. Song, X. Liu, Z. Tang, S. Q. Zang, B. Yang and S. Lu, *Angew. Chem., Int. Ed.*, 2021, **60**, 14091–14099.
29 A. Li, D. Zheng, M. Zhang, B. Wu and L. Zhu, *Langmuir*, 2020, **36**, 8965–8970.
30 L. Zhou, D. Zheng, B. Wu, Y. Zhu and L. Zhu, *ACS Appl. Nano Mater.*, 2019, **3**, 946–952.
31 S. Fleming, S. Debnath, P. W. J. M. Frederix, T. Tuttle and R. V. Ulijn, *Chem. Commun.*, 2013, **49**, 10587–10589.
32 M. B. Avinash and T. Govindaraju, *Nanoscale*, 2014, **6**, 13348–13369.
33 Y. Wang, W. Qi, R. Huang, X. Yang, M. Wang, R. Su and Z. He, *J. Am. Chem. Soc.*, 2015, **137**, 7869–7880.
34 M. Deng, L. Zhang, Y. Jiang and M. Liu, *Angew. Chem., Int. Ed.*, 2016, **55**, 15062–15066.
35 J. Zheng, R. Fan, H. Wu, H. Yao, Y. Yan, J. Liu, L. Ran, Z. Sun, L. Yi, L. Dang, P. Gan, P. Zheng, T. Yang, Y. Zhang, T. Tang and Y. Wang, *Nat. Commun.*, 2019, **10**, 1604.
36 G. Liu, J. Sheng, H. Wu, C. Yang, G. Yang, Y. Li, R. Ganguly, L. Zhu and Y. Zhao, *J. Am. Chem. Soc.*, 2018, **140**, 6467–6473.
37 H. Wu, Y. Zhou, L. Yin, C. Hang, X. Li, H. Agren, T. Yi, Q. Zhang and L. Zhu, *J. Am. Chem. Soc.*, 2017, **139**, 785–791.
38 B. Wu, H. Wu, Y. Gong, A. Li, X. Jia and L. Zhu, *J. Mater. Chem. C*, 2021, **9**, 4275–4280.
39 B. Wu, H. Wu, Y. Zhou, D. Zheng, X. Jia, L. Fang and L. Zhu, *Angew. Chem., Int. Ed.*, 2021, **60**, 3672–3678.
40 B. Adhikari, A. Shah and H. B. Kraatz, *J. Mater. Chem. B*, 2014, **2**, 4802–4810.
41 S. Wang, Y. Zhang, X. Qin, L. Zhang, Z. Zhang, W. Lu and M. Liu, *ACS Nano*, 2020, **14**, 6087–6096.
42 A. M. Smith, R. J. Williams, C. Tang, P. Coppo, R. F. Collins, M. L. Turner, A. Saiani and R. V. Ulijn, *Adv. Mater.*, 2008, **20**, 37–41.
43 N. Zanna, A. Merlettini, G. Tatulli, L. Milli, M. L. Focarete and C. Tomasini, *Langmuir*, 2015, **31**, 12240–12250.
44 J. T. Davis and G. P. Spada, *Chem. Soc. Rev.*, 2007, **36**, 296–313.
45 G. M. Peters, L. P. Skala, T. N. Plank, B. J. Hyman, G. N. Manjunatha Reddy, A. Marsh, S. P. Brown and J. T. Davis, *J. Am. Chem. Soc.*, 2014, **136**, 12596–12599.
46 G. M. Peters, L. P. Skala and J. T. Davis, *J. Am. Chem. Soc.*, 2015, **138**, 134–139.
47 G. M. Peters, L. P. Skala, T. N. Plank, H. Oh, G. N. Reddy, A. Marsh, S. P. Brown, S. R. Raghavan and J. T. Davis, *J. Am. Chem. Soc.*, 2015, **137**, 5819–5827.
48 G. M. Peters and J. T. Davis, *Chem. Soc. Rev.*, 2016, **45**, 3188–3206.
49 T. N. Plank, L. P. Skala and J. T. Davis, *Chem. Commun.*, 2017, **53**, 6235–6238.
50 J. Bai, X. Sun, H. Wang, C. Li and R. Qiao, *J. Org. Chem.*, 2020, **85**, 2010–2018.
51 T. Aggerholm, S. C. Nanita, K. J. Koch and R. G. Cooks, *J. Mass Spectrom.*, 2003, **38**, 87–97.
52 D. Loco, S. Jurinovich, L. D. Bari and B. Mennucci, *Phys. Chem. Chem. Phys.*, 2016, **18**, 866–877.
53 A. Randazzo, G. P. Spada and M. W. da Silva, *Top. Curr. Chem.*, 2013, **330**, 67–86.
54 M. Noh, T. Kim, H. Lee, C.-K. Kim, S.-W. Joo and K. Lee, *Colloids Surf., A*, 2010, **359**, 39–44.
55 I. W. Hamley and V. Castelletto, *Prog. Polym. Sci.*, 2004, **29**, 909–948.
56 K. B. Sutyak, P. Y. Zavalij, M. L. Robinson and J. T. Davis, *Chem. Commun.*, 2016, **52**, 11112–11115.